Journal of
Materials Chemistry

Cite this: DOI: 10.1039/c2jm33757f

www.rsc.org/materials

FEATURE ARTICLE

Understanding experimental characterization of intermediate band solar cells

Antonio Martí,*[a] E. Antolín,[ab] P. G. Linares[a] and A. Luque[a]

Received 11th June 2012, Accepted 24th July 2012
DOI: 10.1039/c2jm33757f

An intermediate band solar cell is a novel photovoltaic device with the potential to exceed the efficiency of single gap solar cells. In the last few years, several prototypes of these cells, based on different technologies, have been reported. Since these devices do not yet perform ideally, it is sometimes difficult to determine to what extent they operate as actual intermediate band solar cells. In this article we provide the essential guidelines to interpret conventional experimental results (current–voltage plots, quantum efficiency, *etc.*) associated with their characterization. A correct interpretation of these results is essential in order not to mislead the research efforts directed towards the improvement of the efficiency of these devices.

Introduction

Intermediate band solar cells (IBSCs) have the potential to exceed the efficiency of single gap solar cells thanks to the absorption of below bandgap energy photons and the extraction of the subsequent photocurrent at high voltage.[1] The absorption of below bandgap energy photons takes place through a set of energy levels, called the intermediate band (IB) located inside the conventional semiconductor gap (Fig. 1). Due to the presence of this band, below the bandgap energy, photons pump electrons from the valence band (VB) to the IB (photons labeled "2") and from the IB to the conduction band (photons labeled "3"). In this way, two below bandgap energy photons create one net electron–hole pair that adds to the ones conventionally generated by the absorption of higher energy photons capable of pumping electrons from the VB to the conduction band, CB (photons labeled "1").

The energy levels that constitute the IB can be created following several approaches, quantum dots[2] and the insertion of appropriate impurities at high concentrations[3] being the main ones that have been taken to practice. This set of energy levels should be formed in such a way that they do not introduce significant non-radiative recombination. This is the reason why, when the theory of the IBSC was formulated, they were called "band" (intermediate band) in order to emphasize that their recombination properties should not be different from those achievable between conventional CB and VB, where radiatively dominated recombination is possible (take for example, the case of GaAs). On the other hand, transport through the IB is not required *a priori* since, as will be seen, the IB is electrically

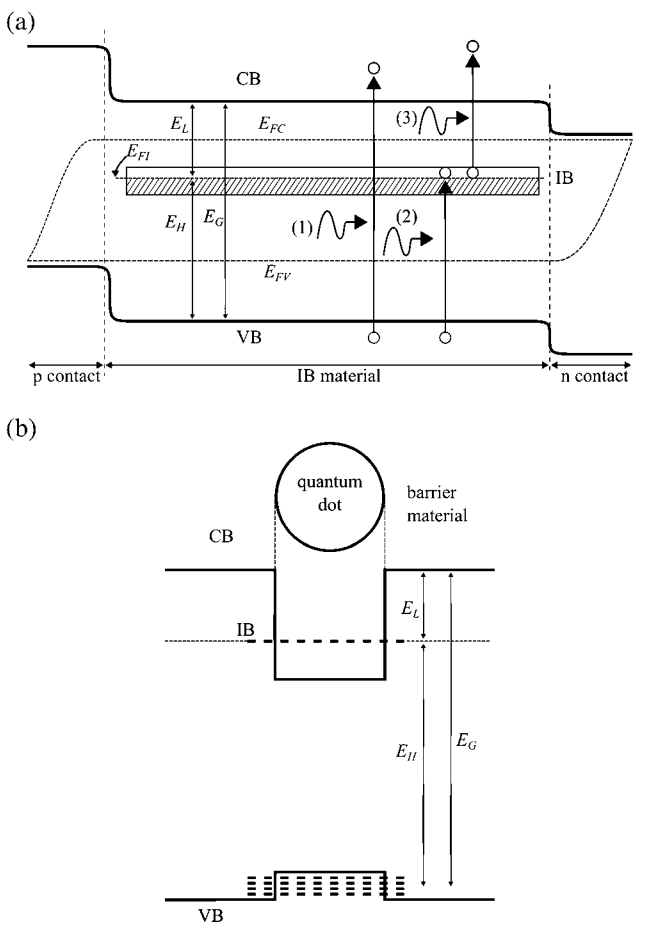

Fig. 1 (a) Simplified band diagram of an IBSC under forward bias and illumination containing also the description of its fundamental operation. (b) Simplified energy band diagram of a QD showing the equivalence with the band structure of an IBSC.

[a]*Instituto de Energía Solar – Universidad Politécnica de Madrid, ETSI Telecomunicación, Ciudad Universitaria sn, 28040 Madrid, Spain. E-mail: amarti@etsit.upm.es*
[b]*Instituto de Microelectrónica de Madrid, CNM (CSIC), c/Isaac Newton 8, PTM, Tres Cantos, 28760 Madrid, Spain*

isolated from the contacts. Because of this, a narrow IB, with potentially high effective masses and low mobility, can be tolerated.

In the case of the implementation with QDs, the energy levels emerge typically from the confinement of the electrons in the potential wells created in the conduction band (Fig. 1b). In this case, radiative generation–recombination from the CB to the confined level and from the confined level to the VB is conceptually possible without the energy levels needing to form an actual band in the sense of the wavefunction of one electron in one dot extending to the neighboring QD. On the other hand, advantages such as the achievement of a more uniform carrier generation in the cell are predicted if a miniband is formed.[4]

Because carrier relaxation between bands is assumed to be a much slower process than carrier relaxation within bands, each band, including the IB, has been associated with its own quasi-Fermi level (E_{FC}, E_{FI} and E_{FV} for the CB, IB and VB respectively) to describe the corresponding carrier concentration in each band. Due to the fact that the intermediate band material is sandwiched in-between two single-gap semiconductors,[5] the IB does not contact the external electrodes and E_{FC} and E_{FV} can split from E_{FI}, leading to a configuration as the one conceptually represented in Fig. 1a. High output voltages in the IBSC are possible because the output voltage, V, relates to the electron and hole quasi-Fermi level split as $eV = (E_{FC} - E_{FV})$ and this is only limited by the total bandgap E_G of the semiconductor.

Fig. 2 shows the ideal current–voltage characteristic of an IBSC based on GaAs as the host semiconductor. Ideal means that only radiative recombination rules the electron transitions between bands. It must be clarified that GaAs is not the optimum material for hosting an IB but its choice for this example is based on its convenience to support the discussions in the forthcoming sections. Plots in Fig. 2 also serve the purpose of illustrating conceptual details related to the operation of an IBSC. When an IB is inserted in GaAs, the resulting ideal cell increases its current but loses voltage significantly when operated at one sun. The current gain is compensated by the voltage loss and the resulting efficiency is only marginally better than that of GaAs without an IB. Notice that this voltage loss takes place even when the cell is assumed to operate in its radiative limit. However, when the same cell is operated under concentrated light, the IBSC preserves its photocurrent enhancement while its open-circuit voltage approaches that of the reference cell. This voltage recovery is what often is referred to as "voltage preservation".

In the paragraphs above we have summarized the main aspects of the IBSC theory so that this paper can be comprehended in a self-contained way. More exhaustive reviews can be found in ref. 6–11.

Several IBSCs have been by now manufactured in practice. Perhaps the one that has been studied the most is that in which the IB is formed with QDs. Notable results have also been obtained at device level with IBSCs based on ZnTe with oxygen[12,13] and GaN_xAs_{1-x}.[14] Since more and more experimental devices are being developed, in the next sections we provide a guide for the correct interpretation of the experimental characterization of these cells since, as we shall see, in some cases (such as the quantum efficiency) this can be counterintuitive. We restrict ourselves to the discussion of the experimental techniques that have already proven useful to characterize some of the existing IBSCs.

Current–voltage characteristics

The current–voltage characteristic at one sun is usually the simplest (when precise spectral calibration is not pursued) measurement available to a solar cell. To start our discussion, Fig. 3 shows an early current–voltage characteristic of an IBSC based on QDs. Even from this single measurement we can gather significant information from the perspective of the operation of an IBSC.

As first observation, the output voltage of the cell with QDs is degraded with respect to that of the GaAs reference cell. This voltage loss was expected to some extent from the results in Fig. 2. However, because the voltage drop is not accompanied by a significant current gain, we must conclude (assuming the rest of the parameters in the reference and the IBSC remain the same) that the voltage loss is mainly due to the introduction of additional non-radiative recombination. On the one hand, the low open-circuit voltage of the GaAs reference cell (about 0.85 V) has already anticipated the presence of non-radiative recombination centers. In ref. 16 it was shown that when these non-radiative

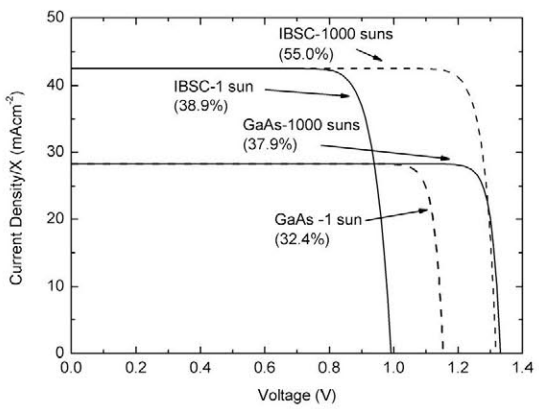

Fig. 2 Ideal current–voltage characteristic of a GaAs cell operating at one sun and at 1000 suns (ASTM G173-03 Direct Normal[15]) and an intermediate band solar cell based on GaAs with the IB located at 0.4 eV from the conduction band also operated at one sun and 1000 suns.

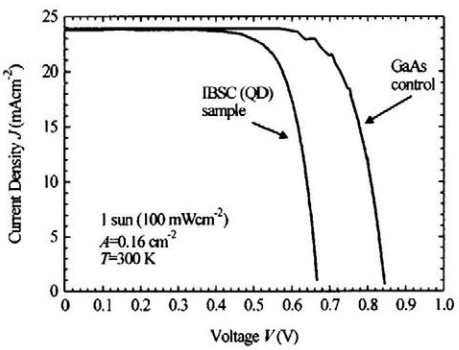

Fig. 3 Current–voltage characteristic of a GaAs reference cell and an InAs/GaAs QD-IBSC not showing evident current improvement but voltage degradation[18] (Copyright American Institute of Physics. Reproduced with permission).

recombination centers are present in the reference cell, their impact on the performance of the corresponding IBSC is usually accentuated. On the other hand, Bailey *et al.*[17] have already reported a solar cell based on QDs with increased photogenerated current over its reference and with an open-circuit voltage close to 1 V (Fig. 4) although they do not appeal to any IBSC effect to explain the result.

Concerning the dark current–voltage characteristics of IBSCs, the effect of voltage recovery has been theoretically predicted[16,19] as showing up as a convergence between the dark current voltage characteristics of the IBSC and its reference without the IB as the injected current increases (Fig. 5). The practical experimental verification of this effect requires devices with low series resistance since this dominates the current–voltage characteristics of the cells at high current densities which would mask the convergence. A way to circumvent series resistance effects in the dark current–voltage characteristic of a solar cell consists of measuring photogenerated current *vs.* open-circuit voltage pairs as the intensity of the illumination on the cell increases. These pairs are equivalent to the dark-current voltage characteristic of the cells without series resistance. If concentrated light is used to provide the high illumination intensity that is required, the use of a flash lamp and careful temperature control is advised in order to minimize the impact of sample overheating so that accurate open-circuit voltage measurements can be obtained. Experimental results concerning this kind of measurement will be discussed in the section Characterization under concentrated light.

Quantum efficiency

The simplest quantum efficiency (QE) measurement consists of illuminating the cell with a calibrated monochromatic photon beam and plotting the current induced in the cell in terms of electrons circulating through the cell divided by the number of incident photons. Examples of this measurement, at different temperatures, are shown in Fig. 6 and correspond to different IBSCs made of InAs quantum dots in GaAs.[20] The approximated bandgap diagram in a cell of this kind is represented in Fig. 7, where three different mechanisms for pumping electrons from the VB to the CB through the IB (not all necessarily adequate in the IBSC context) are also depicted. The interpretation of these quantum efficiency measurements leads us to the conclusions reasoned in the next paragraphs.

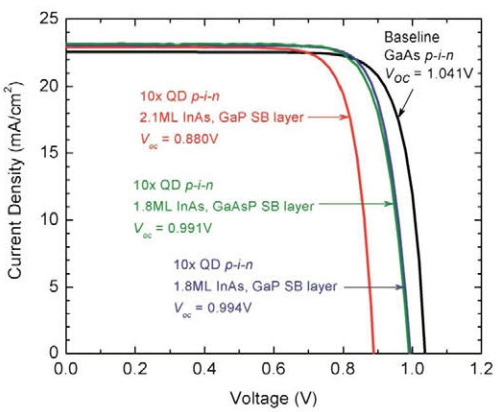

Fig. 4 Current–voltage characteristic of a GaAs reference cell and an InAs/GaAs QD-IBSC showing minimal voltage degradation but current improvement[17] (Copyright American Institute of Physics. Reproduced with permission).

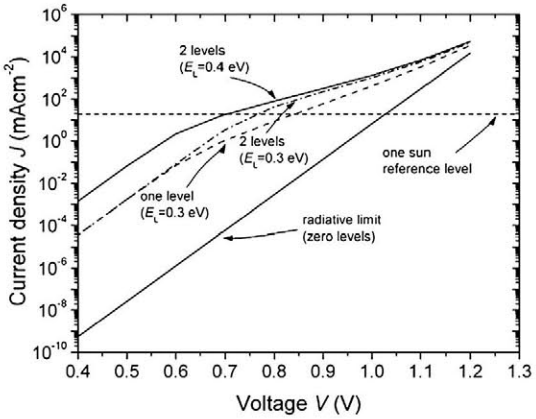

Fig. 5 Ideal dark current–voltage characteristics of an IBSC and its reference showing convergence as the injected current increases. The "zero levels" case corresponds to the reference cell. The "one level" case corresponds to the IBSC. The "2 levels" case corresponds to an IBSC in which an additional energy level appears. The value assumed for the bandgap E_L is also shown[19] (Copyright Elsevier. Reproduced with permission).

First, because the cells are based on GaAs, the total bandgap of the IBSC corresponds to 1.4 eV at room temperature and 1.5 eV at low temperature. Then, in agreement with the IBSC theory, as can be seen, there is production of photocurrent by photons with energy below the bandgap.

Second, because in this measurement the cells are being illuminated by a single monochromatic beam, we need to explain how electrons are finally pumped from the VB to the CB in the below bandgap energy region. It could be that photons pumping electrons from the VB to the IB were also capable of pumping electrons from the IB to the CB (case illustrated in Fig. 7a). However, it could also be that photons were thermally pumped from the IB to the CB (case illustrated in Fig. 7b) or that, through an impact ionization process, two photons would pump electrons from the VB to the IB but then, the energy of one electron recombining back to the VB was transferred to an electron in the IB which is then pumped to the CB (case illustrated in Fig. 7c).[21] Of course, a combination of several of these mechanisms is also possible.

Third, if the mechanism illustrated in Fig. 7a exists, then we have also to acknowledge that there is overlap between the absorption coefficient related to transitions from the IB to the CB (α_{CI}) and the absorption coefficient related to transitions from the VB to the IB (α_{IV}). The ideal performance of the IBSC for an optimal structure requires that either that overlap does not exist or that if it exists, $\alpha_{IV} \gg \alpha_{CI}$ in the energy intervals at which they overlap. Conversely, notice that cells not showing below bandgap response under this quantum efficiency measurement should not be immediately disregarded as not working since, after all, it might happen that they are actually performing ideally! Nevertheless, in the case where $\alpha_{IV} \gg \alpha_{CI}$ light management strategies[22–24] would be required to manufacture an efficient IBSC to compensate for the weak α_{CI}.

Fourth, if electrons are being pumped "thermally" from the IB to the CB, then lowering the temperature of the measurement

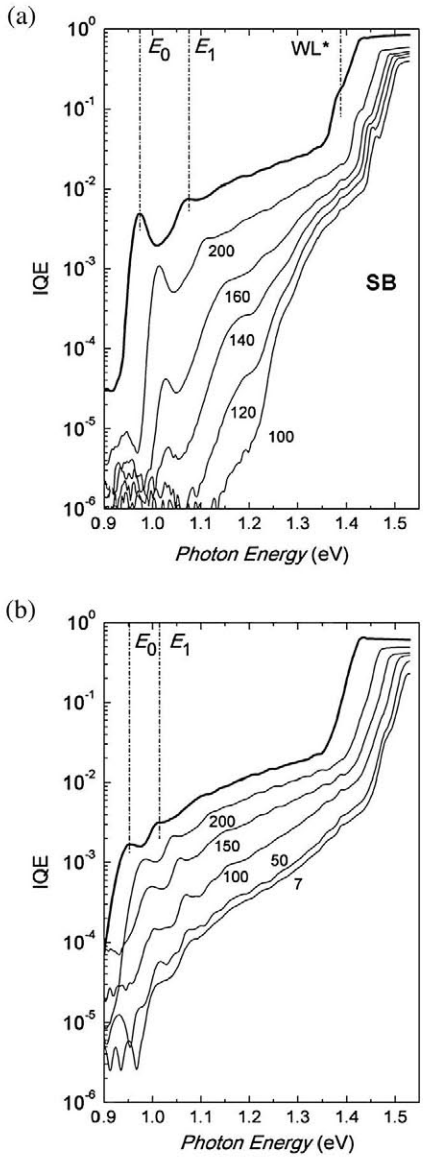

Fig. 6 Example of internal quantum efficiencies measured on InAs/GaAs QD-IBSC showing different behaviors with temperature[20] (Copyright American Institute of Physics. Reproduced with permission).

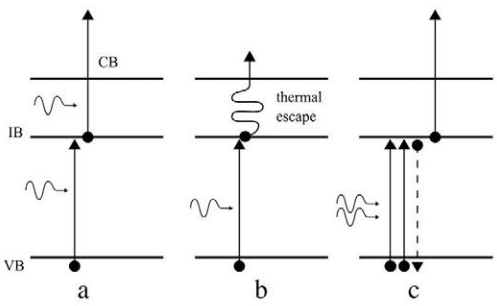

Fig. 7 Simplified electronic structure of an InAs/GaAs QD-IBSC also showing different mechanisms by which a monochromatic beam of sub-bandgap energy photons can pump an electron from the VB to the CB: (left) one photon pumps an electron from the VB to the IB and a second photon pumps an electron from the IB to the CB; (center) thermal escape; (right) impact ionization.

should inhibit the below-bandgap response of the cell. The physical origin of the thermal escape is the existence of non-radiative generation mechanisms and/or the absorption of thermal blackbody radiation.[25] We see that this is the case in the example illustrated in Fig. 6a, where the thermal escape has been almost completely suppressed at 100 K, but it is not in the case in Fig. 6b. In the example in Fig. 6b, the below-bandgap response does not decrease substantially below 50 K. This is interpreted as caused by the existence of a tunneling mechanism that, favored by the fact that the QDs are immersed in an electric field region (Fig. 8), allows electrons to tunnel from the IB to the CB.[20] The reason behind the different performance between both cells in this respect is the different thickness of the GaAs barriers (bulk semiconductor layers that separate the QD layers) in each case (84 nm in the example in Fig. 6a *vs.* 13 nm in the case of Fig. 6b). Either way, the decrease of the below-bandgap response when lowering the temperature implies the existence of a contribution from thermal escape to the pumping of electrons from the IB to the CB that, according to the IBSC theory implies a difficulty in achieving, at room temperature, a quasi-Fermi level split between CB and IB.[26]

Fifth, if the mechanism governing the promotion of electrons from the VB to the CB was impact ionization, there would still be room for efficiencies higher than those of single gap solar cells.[21] However, whether this mechanism is contributing to the quantum efficiency cannot be determined, to our knowledge, from this measurement alone.

Finally, the QE measurement in the IBSC context can be proven useful at least in order to: (a) in those cases in which the short-circuit in the current–voltage characteristic of the cell shows improvement over the reference cell, verify that this improvement is due to a contribution from the below-bandgap response of the cell and not to accidental differences in the response above the bandgap (for example, differences on the quality of the emitter grown on top of the IB material and/or differences in the properties of the antireflecting coatings); (b) assist in the development of more efficient devices by identifying,

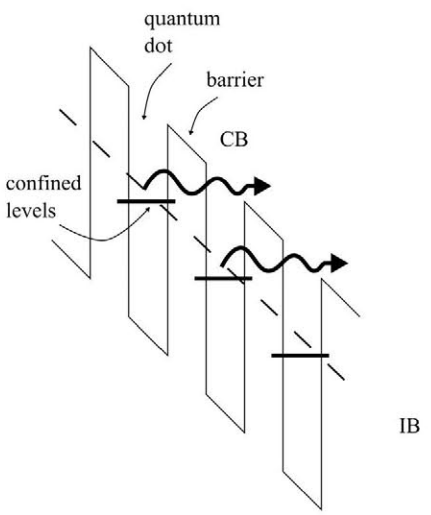

Fig. 8 Illustration of the tunneling mechanism promoting electrons from the IB to the CB. The QDs are assumed to be located at the space charge region.

for example, the appearance of defects due to an inadequate compensation of the strain introduced by the QDs.[27]

Two-photon measurements

Measurements involving two monochromatic beams are adequate in order to determine whether net transitions from the VB to the CB actually involve the absorption of two photons or not. As will be remembered, the contribution of the free energy by two photons is necessary in order to preserve the output voltage of the cell without violating the second law of thermodynamics.[26] Although some variants of the technique are possible, assuming for example a scheme in which the IB–CB gap (E_L) is the smallest and the VB–IB gap (E_H) is the largest sub-bandgap, first the cell is illuminated with photons with energy that is enough to pump electrons from the VB to the IB, but insufficient to pump electrons from the VB to the CB. The output current of the cell is registered. Then, a second beam of photons, this time with energy capable of pumping electrons from the IB to the CB but not as high as to pump electrons from the VB to the IB is added to the first beam. If an increase in photocurrent occurs when this second beam is introduced, then we can conclude that the two-photon process is taking place. This kind of experiment has successfully been carried out in ZnTe:O IBSCs at room temperature.[12,13] However, if at room temperature, the IB to CB transition is saturated by thermal transitions (meaning that thermal transitions have the capability of pumping to the CB all the electrons being pumped to the IB from the VB by the first beam) the incidence of the second photon beam will have no appreciable effect. This has been the case in QD-IBSCs where lowering the temperature has been necessary in addition to the assistance of lock-in techniques to detect the contribution of the IB to CB transition to the two-photon photocurrent.[28] In this case, in order to achieve the maximum sensitivity in the measurement, it is advised that the light that produces the IB to CB transition is chopped while the light producing the VB to CB is kept continuous rather than the other way around.

Characterization under concentrated light

As advanced in the discussions related to Fig. 2, one of the expected effects that the use of concentrated light has on IBSCs is the convergence of the open-circuit voltage of the IBSC and its reference. An interesting experimental technique to show this effect is by registering the photogenerated current *vs.* open-circuit voltage pairs of the cells as the concentration increases. Assuming that the superposition principle is fulfilled, the resulting plot is also an indirect measurement of how the dark current–voltage characteristic of the cells would be without series resistance effects. This dark current should also show this convergence if series resistance would not usually mask this phenomenon.

The convergence in open-circuit voltage has already been experimentally observed in QD-IBSCs based on InAs/GaAs[29] where the open-circuit voltage of the cells with QDs has approached that of the reference cell without QDs at high concentrations (Fig. 9). According to the IBSC theory, in order that voltage recovery becomes possible while getting the current increased, the CB and the IB must each have its own quasi-Fermi

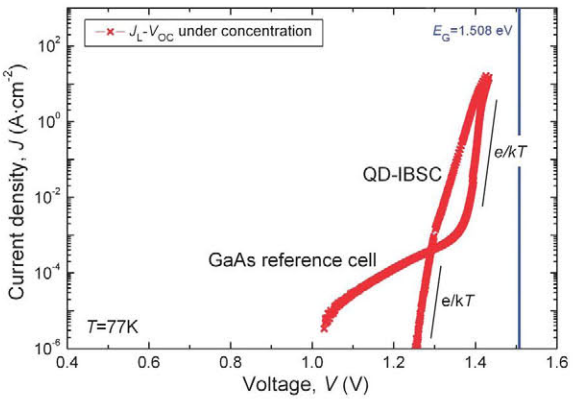

Fig. 9 Photogenerated current *vs.* open-circuit voltage of a QD-IBSC based on InAs/GaAs and its reference.[29] Measurements are made at 77 K. The GaAs bandgap at this temperature is also shown for the reference (Copyright Elsevier. Reproduced with permission).

level. This is possible when the lifetime associated with CB to IB recombination is much larger than the lifetime associated with carrier relaxation within each band. This is not expected to be the case when thermal escape is the dominant process ruling the IB to CB transitions and therefore, lowering the temperature was necessary in order to observe the recovery of the voltage. Consistent with the discussions in the section Quantum efficiency, in those cells in which even by lowering the temperature it has not been possible to avoid electrons transiting from the IB to the CB by mechanisms such as tunneling, the observation of the voltage recovery has not been possible even under strong light illumination[30] (Fig. 10b).

Electroluminescence

Given the fact that three distinguished bands exist in the IBSC, three recombination processes are also associated with transitions from the CB to the IB, from the IB to the VB and from the CB to the VB. If a fraction of this recombination is radiative, it should be detected as photon emission at three different wavelengths.[31] Under this mode of operation, the IBSC would operate as a three color light emitting diode, and at the same time it would provide additional proof of its operation according to the IBSC principles. To our knowledge, this three color emission has only been reported in GaN_xAs_{1-x} based intermediate band solar cells[14] (Fig. 11). Electroluminescence, in combination with QE, has also been used[32] to measure the quasi-Fermi level split between CB and IB in dark conditions and under conditions of high current injection at nominally room temperature. A quasi-Fermi level split above 150 meV was found at an excitation of 5 A cm^{-2}. The measurement has been criticized in ref. 33 which argues that the overheating of the sample might have affected the results.

EL characterization has also been used to complement the study of voltage preservation in QD-IBSCs at low temperatures. Fig. 12 shows the EL spectra of a GaAs reference sample (left) and of an InAs/GaAs QD-IBSC, from ref. 34. This QD-IBSC prototype is similar to the one used for the measurements in Fig. 6a and 10a. From the previous sections it was concluded that these devices do not behave according to the IBSC principles at

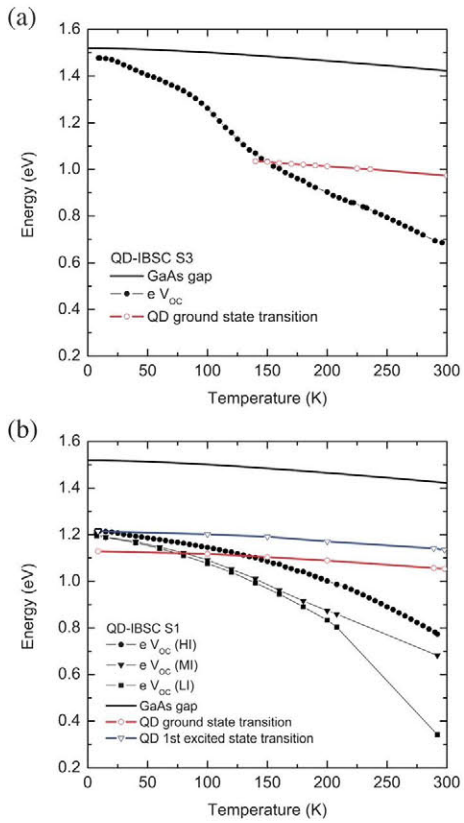

Fig. 10 Open-circuit voltage as a function of temperature for two examples of QD-IBSCs. Energy levels, including the value of the bandgap, are also shown for reference. In (a), corresponding to a cell in which it is possible to suppress the thermal escape, the open-circuit voltage (multiplied by the electron charge) recovers and approaches the bandgap of the cell at low temperature. In (b), in which it was not possible to suppress the electron escape from the IB to the CB due to the existence of tunneling mechanism, the voltage remains limited by the gap between the IB and the VB[30] (Copyright IEEE. Reproduced with permission).

room temperature due to the thermal connection between IB and CB, but they do behave as an IBSC at low temperatures. Consequently, the EL spectra shown in Fig. 12 (right) are dominated by IB–VB recombination at high temperatures

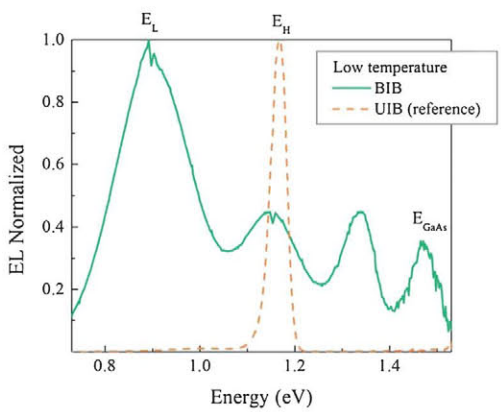

Fig. 11 Electroluminescence spectrum of an GaN_xAs_{1-x} IBSC showing the peaks associated with the CB to IB transition (E_L) and with the IB to VB transition (E_H)[14] (Copyright American Physical Society. Reproduced with permission).

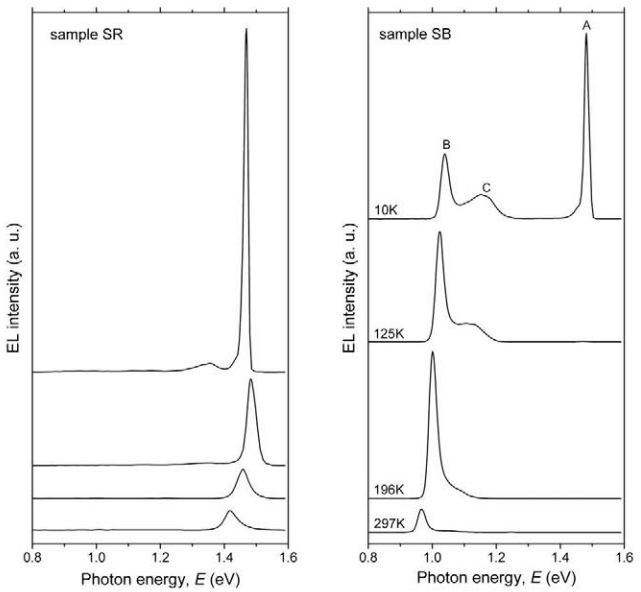

Fig. 12 Electroluminescence spectra of a GaAs reference cell (left) and a QD-IBSC (right) at different temperatures. Peak heights have not been normalized. From ref. 34 (Copyright Elsevier. Reproduced with permission).

($E_H \sim 1$ eV) because CB–IB carrier relaxation is too fast. At low temperatures, once voltage preservation is enabled, the EL spectrum is that expected from a proper IBSC: both peaks at E_H and E_G are observed (E_L is beyond the detection range in this measurement). It has to be noted that a PL measurement cannot be used in general to do this characterization because the luminescence from the cell's emitter can induce false conclusions.[34]

Characterization at wafer level

The experimental techniques reported in the previous sections require the implementation of IBSCs at the device level. Implementing the cell at device level demands not only the synthesis of the IB material but also the technology related to the creation of the suitable emitters (layers that sandwich the IB material). The creation of these emitters can be a problem on its own. The effort to develop them might not be necessary if suitable characterization techniques would be able to tell us in advance if the intermediate band material candidate actually has potential to produce a high efficiency solar cell device. Current experience related to the characterization of IBSC material candidates at wafer level (that is, prior to the manufacturing of an actual solar cell) is still limited.

In this context, photoreflectance has been used in ref. 13, 35, and 36 to confirm the appearance of an IB in GaNAsP quaternary alloys, II–VI diluted oxide semiconductors and ZnTe:O.

Measurements of light absorption have been used to report the existence of an IB in V substituted In_2S_3 (ref. 37) by identifying the absorption thresholds associated with each of the transitions involved. Photoconductive decay lifetime measurements have been used to show lifetime improvement in titanium implanted silicon wafers[38] followed by pulsed laser melting (Fig. 13) as predicted by the IBSC theory when the impurity concentration increases and non-radiative recombination begins to be inhibited

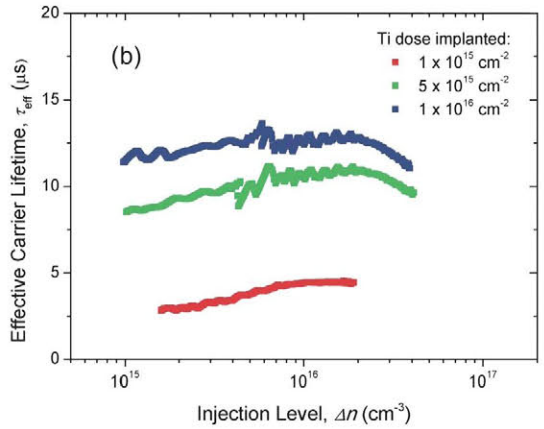

Fig. 13 Lifetime improvement in Ti implanted silicon wafers[38] as Ti concentration increases (Copyright American Institute of Physics. Reproduced with permission).

due to the formation of an intermediate band. In addition, Hall effect measurements have been used to determine the conductivity of this band[39,40] and therefore, indirectly, also demonstrating its formation.

Fourier Transform Infrared Spectroscopy (FTIR) has been applied to the characterization of photon absorption between the IB and the CB in QD samples at room temperature[41,42] although the absorption signatures reported probably lack sharpness and a quantitative analysis could not be provided yet. This technique is especially interesting when studying the effect of QD doping on the IB–CB absorption strength.[42]

Conclusions

Experiments have demonstrated the main physical principles involved in the operation of intermediate band solar cells. Illumination with two photon monochromatic sources has allowed demonstration of the absorption of two below-bandgap energy photons to produce one net electron hole pair in the InAs/GaAs QD intermediate band (at low temperature) and ZnTe:O solar cells (at room temperature). Concentration measurements have allowed voltage preservation in QD-IBSCs (at low temperatures) to be demonstrated. If practical devices are pursued, efforts should be devoted towards the demonstration of these effects at room temperature (in the cases in which this has not been demonstrated) as well as to make them effectively contribute to the enhancement of the cell efficiency.

Apparently trivial measurements such as current–voltage characteristics or quantum efficiency measurements should be interpreted carefully. For example, as has been explained in the text, a QE measurement with a single photon beam not showing a below-bandgap response does not necessarily imply that the cell is not working according to the physical principles of the IBSC since paradoxically, the very ideal IBSC should not show that response. The application of characterization techniques capable of determining the optoelectronic properties of IB materials (for example, light absorption) before the actual manufacturing of a device might increase the development of successful devices by ruling out at early stages those without the potential for producing efficient devices.

Acknowledgements

This work has been supported by the 7th Framework European Project NGCPV (Grant number 283798). EA acknowledges a *Juan de la Cierva* Post-Doctoral Fellowship (JCI-2011-10639) from the Spanish Ministry of Science.

Notes and references

1 A. Luque and A. Martí, *Phys. Rev. Lett.*, 1997, **78**, 5014–5017.
2 A. Martí, L. Cuadra and A. Luque, *Conference Record of the Twenty-Eighth IEEE Photovoltaic Specialists Conference, 2000*, 2000, pp. 940–943.
3 A. Luque, A. Martí, E. Antolín and C. Tablero, *Phys. B*, 2006, **382**, 320–327.
4 A. Martí, L. Cuadra and A. Luque, *IEEE Trans. Electron Devices*, 2002, **49**, 1632–1639.
5 A. Luque and A. Martí, *Progr. Photovolt.: Res. Appl.*, 2001, **9**, 73–86.
6 A. Martí, L. Cuadra and A. Luque, in *Next Generation Photovoltaics: High Efficiency Through Full Spectrum Utilization*, ed. A. Martí and A. Luque, Institute of Physics Publishing, Bristol, 2003, pp. 140–162.
7 A. Martí and A. Luque, in *Next Generation of Photovoltaics: New Concepts*, ed. A. B. Cristóbal, A. Martí and A. Luque, Springer Series in Optical Sciences, Berlin, 2012.
8 A. Martí, C. R. Stanley and A. Luque, in *Nanostructured Materials for Solar Energy Conversion*, ed. T. Soga, Elsevier, 2006.
9 A. Luque, A. Martí and C. R. Stanley, *Nat. Photonics*, 2011, **9**, 137–138.
10 A. Luque and A. Martí, *Adv. Mater.*, 2010, **22**, 160–174.
11 E. Antolín, A. Martí and A. Luque, in *VLSI Photonics*, CRC, 2010.
12 W. Wang, A. S. Lin and J. D. Phillips, *Appl. Phys. Lett.*, 2009, **95**, 011103.
13 T. Tanaka, K. M. Yu, A. X. Levander, O. D. Dubon, L. A. Reichertz, N. Lopez, M. Nishio and W. Walukiewicz, *Jpn. J. Appl. Phys.*, 2011, **50**, 3.
14 N. Lopez, L. A. Reichertz, K. M. Yu, K. Campman and W. Walukiewicz, *Phys. Rev. Lett.*, 2010, **106**, 028701.
15 Renewable Resource Data Centre; NREL, http://rredc.nrel.gov/solar/spectra/am1.5/. accessed 13 May 2012. (Archived by WebCite® at http://www.webcitation.org/67cfYnJUz).
16 A. Luque, P. G. Linares, E. Antolin, I. Ramiro, C. D. Farmer, E. Hernandez, I. Tobias, C. R. Stanley and A. Marti, *J. Appl. Phys.*, 2011, **111**, 044502–044512.
17 C. G. Bailey, D. V. Forbes, R. P. Raffaelle and S. M. Hubbard, *Appl. Phys. Lett.*, 2011, **98**, 163105.
18 A. Luque, A. Marti, C. Stanley, N. Lopez, L. Cuadra, D. Zhou, J. L. Pearson and A. McKee, *J. Appl. Phys.*, 2004, **96**, 903–909.
19 A. Martí, E. Antolín, E. Cánovas, N. López, P. G. Linares, A. Luque, C. R. Stanley and C. D. Farmer, *Thin Solid Films*, 2008, **516**, 6716–6722.
20 E. Antolin, A. Marti, C. D. Farmer, P. G. Linares, E. Hernandez, A. M. Sanchez, T. Ben, S. I. Molina, C. R. Stanley and A. Luque, *J. Appl. Phys.*, 2010, **108**, 064513.
21 A. Luque, A. Martí and L. Cuadra, *IEEE Trans. Electron Devices*, 2003, **50**, 447–454.
22 A. Luque, A. Marti, M. J. Mendes and I. Tobias, *J. Appl. Phys.*, 2008, **104**, 113118.
23 M. J. Mendes, A. Luque, I. Tobias and A. Marti, *Appl. Phys. Lett.*, 2009, **95**, 071105.
24 A. Mellor, I. Tobías, A. Martí, M. J. Mendes and A. Luque, *Prog. Photovoltaics*, 2011, **19**(6), 676–687.
25 A. Luque, A. Marti, E. Antolin, P. G. Linares, I. Tobias and I. Ramiro, *AIP Adv.*, 2011, **1**, 022125–022126.
26 A. Luque, A. Martí and L. Cuadra, *IEEE Trans. Electron Devices*, 2001, **48**, 2118–2124.
27 A. Marti, N. Lopez, E. Antolin, E. Canovas, A. Luque, C. R. Stanley, C. D. Farmer and P. Diaz, *Appl. Phys. Lett.*, 2007, **90**, 233510–233513.
28 A. Martí, E. Antolin, C. R. Stanley, C. D. Farmer, N. Lopez, P. Diaz, E. Canovas, P. G. Linares and A. Luque, *Phys. Rev. Lett.*, 2006, **97**, 247701–247704.
29 P. G. Linares, A. Martí, E. Antolín, C. D. Farmer, I. Ramiro, C. R. Stanley and A. Luque, *Sol. Energy Mater. Sol. Cells*, 2011, **98**, 240–244.

30 E. Antolin, A. Marti, P. G. Linares, I. Ramiro, E. Hernandez, C. D. Farmer, C. R. Stanley and A. Luque, in *Photovoltaic Specialists Conference (PVSC), 2010 35th IEEE*, 2010, pp. 000065–000070.
31 N. Ekins-Daukes, C. Honsberg and M. Yamaguchi, *Proc. of the 31st IEEE Photovoltaic Specialists Conference*, 2005, pp. 49–54.
32 A. Luque, A. Marti, N. Lopez, E. Antolin, E. Canovas, C. Stanley, C. Farmer, L. J. Caballero, L. Cuadra and J. L. Balenzategui, *Appl. Phys. Lett.*, 2005, **87**, 083505.
33 A. A. Abouelsaood, M. Y. Ghannam and J. Poortmans, *Prog. Photovoltaics*, 2011, DOI: 10.1002/pip.1192.
34 I. Ramiro, E. Antolín, P. G. Linares, E. Hernández, A. Martí, A. Luque, C. D. Farmer and C. R. Stanley, *Energy Procedia (European materials research Society Conference, Symp. Advanced Inorganic materials and Concepts for photovoltaics)*, 2011, pp. 117–121.
35 K. M. Yu, W. Walukiewicz, J. W. Ager, D. Bour, R. Farshchi, O. D. Dubon, S. X. Li, I. D. Sharp and E. E. Haller, *Appl. Phys. Lett.*, 2006, **88**, 092110–092113.
36 K. M. Yu, W. Walukiewicz, J. Wu, W. Shan, J. W. Beeman, M. A. Scarpulla, O. D. Dubon and P. Becla, *Phys. Rev. Lett.*, 2003, **91**, 246403–246404.
37 R. Lucena, I. Aguilera, P. Palacios, P. Wahnón and J. C. Conesa, *Chem. Mater.*, 2008, **20**, 5125–5151.
38 E. Antolin, A. Marti, J. Olea, D. Pastor, G. Gonzalez-Diaz, I. Martil and A. Luque, *Appl. Phys. Lett.*, 2009, **94**, 042115.
39 G. Gonzalez-Díaz, J. Olea, I. Mártil, D. Pastor, A. Martí, E. Antolín and A. Luque, *Sol. Energy Mater. Sol. Cells*, 2009, **93**, 1668–1673.
40 J. Olea, M. Toledano-Luque, D. Pastor, E. San-Andres, I. Martil and G. Gonzalez-Diaz, *J. Appl. Phys.*, 2011, **107**, 5.
41 N. López, M. Burhan, C. Christofides, C. Farmer, P. Díaz, E. Antolín, E. Cánovas, C. Stanley, A. Martí and A. Luque, in *Proc. of the 21st European Photovoltaic Solar Energy Conference*, WIP, Munich, 2006, pp. 385–388.
42 V. Popescu, G. Bester, M. C. Hanna, A. G. Norman and A. Zunger, *Phys. Rev. B: Condens. Matter Mater. Phys.*, 2008, **78**, 205321.